2010

Climate change impacts on water demand and salinity in California's irrigated agriculture

Gerrit Schoups

Edwin P. Maurer
Santa Clara University, emaurer@scu.edu

Jan Hopmans

Climate change impacts on water demand and salinity in California's irrigated agriculture

G. Schoups[1], E.P. Maurer[2], and J.W. Hopmans[3*]

[1] Department of Water Management, Delft University of Technology, Stevinweg 1, P.O. Box 5048, 2600 GA Delft, The Netherlands, phone: +31-15-2784909, email: g.h.w.schoups@tudelft.nl

[2] Civil Engineering Department, Santa Clara University, 500 El Camino Real, Santa Clara, CA 95053, phone: +1-408-554-2178, email: emaurer@engr.scu.edu

[3] Department of Land, Air and Water Resources, University of California, 1 Shields Ave., Davis, CA 95616, phone: +1-530-752-3060, email: jwhopmans@ucdavis.edu

[*]Corresponding author: jwhopmans@ucdavis.edu

ABSTRACT

This paper examines potential regional-scale impacts of climate change on sustainability of irrigated agriculture, focusing on the western San Joaquin Valley in California. We consider potential changes in irrigation water demand and supply, and quantify impacts on the hydrologic system, soil and groundwater salinity with associated crop yield reductions. Our analysis is based on archived output from General Circulation Model (GCM) climate projections through 2100, which were downscaled to the 1,400 km^2 study area. We account for uncertainty in GCM climate projections by considering two different GCM's, each using three greenhouse gas emission scenarios. Significant uncertainty in projected precipitation creates large uncertainty in surface water supply, ranging from a decrease of 26% to an increase of 14% in 2080-2099. Changes in projected irrigation water demand ranged from a decrease of 13% to an increase of 3% at the end of the 21st century. Greatest demand reductions were computed for the dry and warm scenarios, because of increased land fallowing with corresponding decreased total crop water requirements. A decrease in seasonal crop ET by climate warming, despite an increase in evaporative demand, was attributed to faster crop development with increasing temperatures. Simulations of hydrologic response to climate-induced changes suggest that the salt-affected area will be slightly expanded. However, irrespective of climate change, salinity is expected to increase in downslope areas, thereby limiting crop production to mostly upslope areas of the simulation domain. Results show that increasing irrigation efficiency may be effective in controlling salinization, by reducing groundwater recharge and improving soil drainage, and in mitigating climate warming effects, by reducing the need for groundwater pumping to satisfy crop water requirements.

1. Introduction

Potential impacts of global climate change on food production need to be considered to ensure food security for the world's growing population (Schmidhuber and Tubiello, 2007). Impact assessment is especially important for irrigated agriculture, as it supports a large part of the world's food supply, while being vulnerable to water scarcity (Rosegrant and Cline, 2003). Specifically, irrigated lands produce more than 40% of the world's food and account for almost 90% of global water consumption (Döll and Siebert, 2002).

Climate change in the 21st century is expected to affect crop productivity (Rosenzweig and Hillel, 1998; Cline, 2007), irrigation water demand (Döll, 2002), and water supply (Kundzewicz et al., 2007). Crop yields may either increase due to stimulated biomass production with higher CO_2 concentrations, i.e. CO_2 fertilization, or may decrease due to rising air temperatures (Rosenzweig and Hillel, 1998). Early greenhouse experiments suggested that the CO_2 fertilization effect may be significant. However, more recent results from Free-Air CO_2 Enrichment (FACE) trials under field conditions indicate that previous greenhouse studies over-estimated the effect of CO_2 fertilization (Long et al., 2006). A recent study by Cline (2007) projects an overall negative effect of climate change on global crop production, with more severe production losses in the warm climates of Africa, India, and South America.

Climate change is expected to affect irrigation water demand through shifts in precipitation, temperature, and crop transpiration. Döll (2002) projected an increase in water demand for half of the world's irrigated areas, due to increased crop transpiration at higher temperatures and decreased precipitation in some areas. However, two additional factors that may affect water demand were not considered. First, faster crop development at higher temperatures will shorten growing seasons (Ritchie and NeSmith, 1991), resulting in reduced *seasonal* water demand, but potentially increased *annual* water demand when shorter growing seasons allow multiple cropping. Second, higher atmospheric CO_2 concentrations lead to decreases in leaf stomatal conductance, thereby reducing crop transpiration (Kimball et al., 2002). However, this is only significant in C_4 crops, as increased leaf production in C_3 crops is expected to offset decreases in leaf stomatal conductance (Ainsworth and Rogers, 2007).

When evaluating climate change impacts on irrigated agriculture, one must also consider irrigation water supplies from rivers and aquifers. Changes in precipitation, temperature, and evaporation are expected to alter river runoff and surface water supplies (Kundzewicz et al., 2007). Generally speaking, runoff is likely to decrease in semi-arid regions that depend on irrigation for crop production, such as the western United States and the Mediterranean basin (Milly et al., 2005). Furthermore, areas that depend on snowmelt are particularly vulnerable to rising temperatures and shifts in runoff seasonality (Barnett et al., 2005). Reductions in surface water supply may in turn put increased pressure on limited groundwater resources, leading to risks of groundwater depletion (Alley et al., 2002), land subsidence (Galloway et al., 1999), and resource degradation by soil and groundwater salinization (Ghassemi et al., 1995; Moench, 2004; Vlek et al., 2008). Coastal aquifers are especially vulnerable in that respect, due to risks of saltwater intrusion as sea level rises (Sherif and Singh, 1999). On the other hand, a climate-driven increase in groundwater use could be beneficial, by reducing dependence on variable surface water supplies (Schoups et al., 2006), and by improving soil drainage conditions in areas affected by shallow water tables (Belitz and Phillips, 1995).

The implication is that climate change assessments for irrigated agriculture should not only consider changes in water demand and supply, but should also account for cascading effects on the regional hydrologic system, including soils, aquifers, and rivers. In this paper we present such a regional-scale analysis for an area in California's San Joaquin Valley.

In a comprehensive review by Hayhoe et al. (2004), projections from various climate models for a range of emission scenarios were downscaled to evaluate potential hydrological and agricultural impacts in California. General trends for the 21st century include (i) an increase in annual average temperatures, (ii) a decrease in precipitation in the Central Valley, (iii) an increase in heat wave frequency and intensity, and (iv) a substantial reduction in snow pack in the Sierra Nevada Mountains, causing a shift to earlier runoff. Such changes are already apparent in historical records in the western United States, and can be linked to human-induced global warming (Barnett et al., 2008). Vicuna et al. (2007) concluded that seasonal shifts in runoff could diminish water deliveries from the Central Valley Project's (CVP) reservoirs to farms in the San Joaquin Valley by almost 30%, but realized that variation among climate scenarios was large.

Though it is generally believed that warming will increase crop transpiration (CA-DWR, 2006; CA-EPA, 2006; Lobell et al., 2006), few studies have quantified climate change impacts on water demand for California's irrigated agriculture within a broad hydrologic context, considering soil and groundwater salinity and groundwater pumping effects to balance expected reduced surface water supplies. This paper presents a quantitative analysis of the potential effects of 21st century climate change on the sustainability of irrigated agriculture in California's Central Valley, focusing on a 1,400 km^2 study area located in the western San Joaquin Valley (Figure 1). We calculate changes in irrigation water demand, water supply, and groundwater pumping, and evaluate hydrologic responses such as groundwater levels and salinity, with implications for land subsidence and reduced crop yields due to increased soil salinity. Uncertainty in our projections is accounted for by considering a range of climate change scenarios.

2. Methodology

To quantify potential climate change impacts, we consider three greenhouse gas (GHG) emission scenarios, namely SRES B1 (low), A2 (mid-to-high) and A1fi (high). These scenarios largely bracket the range of IPCC's nonintervention future emissions projections, with atmospheric CO_2 concentrations for B1, A2, and A1fi reaching 550, 850, and 970 ppm, respectively by 2100 (IPCC, 2007). Following Hayhoe et al. (2004), we used the output of two General Circulation Models (GCMs), i.e. the National Center for Atmospheric Research-Department of Energy Parallel Climate Model (PCM, Washington et al., 2000), and the U.K. Met Office Hadley Centre Climate Model version three (HadCM3, Gordon et al., 2002). Archived output from these two GCMs for each of the three GHG emission scenarios is used to extract precipitation and air temperature projections for California at a spatial resolution of about 300 km.

Because the spatial resolution of GCM output is large relative to the study area (~30 km across, Figure 1), we employ a downscaling method to develop irrigation district scale climate projections. We applied the empirical statistical downscaling method of Wood et al. (2002; 2004), which has been tested and widely applied (e.g. Barnett et al., 2008; Cayan et al., 2008; Maurer, 2007; Van Rheenen et al., 2004) to downscale climate variables to a 1/8 degree (~12 km) spatial scale. The method comprises two steps. The first step is a bias-correction that uses quantile mapping (Panofsky and Brier, 1968) to adjust monthly GCM simulated precipitation and temperature to statistically match (i.e. yielding identical probability density functions) observations for 1960-1999 aggregated to the GCM scale. The same quantile mapping was applied to 21st century GCM projections, so that while the statistics of observations are reproduced for the late 20th century, both the mean and variability of future climate can evolve according to GCM projections. Second, a spatial downscaling step interpolates monthly anomalies at the GCM scale onto a 1/8 degree grid, and these are applied to observations to produce fine-scale GCM projections of temperature and precipitation.

Starting from these climate scenarios, our regional impact study analyzes future changes in (1) irrigation water demand and (2) irrigation water supply, and (3) evaluates impacts of these changes on the regional hydrology.

2.1. Irrigation water demand

Annual irrigation water demand or requirement *IR* can be expressed as the sum of water needs for all crops,

$$IR = \sum_c A_c \frac{ET_c - P_c}{IE_c} \qquad (1)$$

where c is a crop index, ET_c is crop evapotranspiration (ET), P_c is effective precipitation, IE_c is irrigation efficiency, which accounts for conveyance and leaching losses, and A_c is areal crop fraction. Effective precipitation (P_c) was computed from bias-corrected/downscaled GCM precipitation projections, whereas we considered two irrigation efficiency (IE_c) scenarios. Most crops are irrigated by gravity-systems, with IE_c values between 65 and 80%, depending on water table depth (Belitz and Phillips, 1995). As potential cuts in surface water supply may stimulate adoption of more efficient irrigation technology, we consider two scenarios, namely (i) no change in irrigation efficiency, and (ii) a uniform increase to 90% irrigation efficiency through technological adaptation.

Climate directly and indirectly affects crop ET (ET_c). First, evaporative demand changes as a function of atmospheric conditions such as temperature, relative humidity, net radiation, and wind speed. We quantify this by estimating reference ET (ET_{ref}). based on the ASCE-EWRI standardized equation (ASCE-EWRI, 2004), which is an adaptation of the Penman-Monteith equation for a short reference crop. Climate data used in this equation are based on downscaled GCM projections of temperature and precipitation for California, from which we obtained estimates of relative humidity and radiation. Wind speed is estimated from the NCEP/NCAR reanalysis (Kalnay et al., 1996). A similar approach was developed by Thornton et al. (2000), and successfully applied by Maurer et al. (2002) and Cayan et al. (2008). Figure 2 shows that reference ET in the study area can be correctly estimated with this method using only data on precipitation and temperature.

Climate also indirectly affects crop development by changing growing conditions, of ambient CO_2 levels and air temperature. Effects of increased CO_2 levels on ET_c will depend on photosynthetic pathway. For C_3 crops, an increase in biomass production will offset a decrease in stomatal leaf conductance with increasing atmospheric CO_2 (Ainsworth and Rogers, 2007), resulting in no or small effect on crop ET. The response of C_4 crops is dominated by a reduction in stomatal conductance, resulting in larger ET reductions (Kimball et al., 2002). However, C_4 crops (sorghum and corn) only make up about 1% of all crops in the study area, so that we can assume no effect of CO_2 on crop development, and used daily crop coefficients from Snyder et al. (1989) to calculate ET_c as a function of projected ET_{ref}. In addition, GCM-based temperature projections were used to evaluate temperature effects on crop development and ET_c. This was done by expressing length of crop development stages in degree-days (*DD*) instead of days (Ritchie and NeSmith, 1991), with *DD* computed as a piecewise linear function of average daily temperature (Boote et al., 1998). In this model, no crop development takes place, and *DD* = 0, below a lower threshold temperature T_l and above a high threshold T_u due to heat stress. Maximum crop development is occurring between temperatures T_{opt1} and T_{opt2}, with linear crop growth or *DD* between temperature ranges of T_l and T_{opt1} and between T_{opt2} and T_u. Threshold temperatures T_l = 7°C, T_{opt1} = 30°C, T_{opt2} = 35°C, and T_u = 45°C were obtained by Boote et al. (1998) for a soybean crop, and were used for all crops in the study area as they corresponded well with values of T_l = 8°C and T_{opt1}= 32°C reported by Ritchie and NeSmith (1991), and used by Schlenker et al. (2007) for crops in California. Similarly, Crafts-Brandner and Salvucci (2000) observed heat stress in cotton, a major crop in the study area, at leaf temperatures above 35°C.

We considered three types of land use (A_c) change, namely (i) changes in cropping patterns, (ii) land fallowing, and (iii) land retirement. For California, Howitt et al. (2003) projected a general shift in cropping pattern by 2100 for a range of climate change scenarios, from cotton and grain crops to high-value crops such as vegetables and fruit. This shift was attributed to increased demand for high-value crops, caused by anticipated population growth. To allow for cropping changes, we calculated irrigation water requirements for two cropping scenarios: (i) a gradual demand-driven shift to high-value crops, as suggested by Howitt et al. (2003), and (ii) no change in current cropping patterns. Farmers may respond to cuts in surface water supplies by temporarily taking land out of production by land fallowing, for example when groundwater is unavailable. For each water district in the study area, we used a linear regression relation between land fallowing acreage and surface water supplies for the 1988-1997 period, to project future land fallowing for the range of climate change scenarios, assuming no future investment in additional groundwater pumping capacity. Lastly, land degradation by soil salinization may result in permanent land retirement, as almost 100,000 acres of agricultural land was retired in 2006 in the western SJV (Figure 1; Russ Freeman, Westlands Water District, pers. comm., 2007). We computed future soil salinization under various climate change scenarios and identified additional land acreage that may be retired by 2100.

2.2. Irrigation water supply

Irrigation water requirement or demand, *IR*, can be met by two main sources, namely (i) imported surface water supply *SW*, and (ii) local groundwater supply *GW*, such that $IR = SW + GW$. Given projections in surface water supply (see next paragraph), annual groundwater supply (*GW*) was computed from this water budget. Possible implications of excessive groundwater pumping, such as land subsidence and soil salinization were assessed by simulating hydrologic system responses (section 2.3.).

Surface water supplies were estimated based on the results of Vicuna et al. (2007). For each climate scenario, we generated annual surface water supply time series that account for long-term water supply trends due to climate change, and that preserve historical short-term statistics, such as variance, auto-correlation, and cross-correlation of historical water supply records for each water district within the study area. We calculated annual surface water supply as the sum of a long-term average, which evolves according to climate change projections in each scenario, and a random fluctuation, which reflects short-term deviations from the mean, or

$$SW_y = \mu_y + d_y \tag{2}$$

where SW_y is water supply in year y, μ_y is a low-frequency term, and d_y is a high frequency term. The low-frequency term is calculated based on average precipitation P from the previous n (= 30) years,

$$\mu_y = f\left(\sum_{i=0}^{n-1} \frac{P_{y-i}}{n}\right) \tag{3}$$

where f is based on a correlation between projected changes in precipitation for the study area and surface water supplies projected by Vicuna et al. (2007). Deviations d_y from the mean μ_y are simulated using a first-order (lag one) auto-regressive model for each of the 14 irrigation districts of the study area (Figure 1), or,

$$d_y = \rho\, d_{y-1} + \varepsilon_y \tag{4}$$

where ρ is a first-order (lag-one) auto-correlation coefficient, estimated from the historical record, and ε_y is the observed deviation from the mean for a randomly selected year from the historical record (1973-1997). This resampling procedure ensures that cross-correlations of water supply between districts were preserved in the future supply scenarios. For example, water supply during droughts often depends on the strength of a district's water right, leaving districts with weak water rights typically more affected by water cuts compared to districts with strong water rights.

2.3. Hydrologic response

Schoups et al. (2005) developed and calibrated a hydro-salinity model for the study area using historical data from 1940 to 1997. The model extent is depicted in Figure 1 which is discretized horizontally into a regular spatial grid with a resolution of 800 m, and vertically into 17 layers. The model solves three-dimensional variable saturated subsurface flow and salt transport, and accounts for chemical reactions, in particular gypsum dissolution-precipitation, affecting salt concentrations. Numerical solutions are obtained with the MODHMS code. Please refer to Schoups et al. (2005) for more details. We used their final simulation results of 1997 to perform simulations for each climate change scenario during 1998-2099, with a focus on changes in groundwater levels, soil and groundwater salinity, and impacts on crop yield and land subsidence. Following Schoups et al. (2005), boundary conditions (irrigation, crop ET, precipitation) and stresses (groundwater pumping) were specified annually for each numerical grid cell. Groundwater flow across the north-eastern boundary was simulated using a general head boundary condition, such that flow depends on hydraulic gradients between simulated groundwater levels in the model domain and specified groundwater levels just east, and outside, of the model domain. Since it is not clear how groundwater levels east of the model domain will evolve in the future, we set them equal to historically observed values. Finally, in order to simulate effects of pumping on groundwater levels, we extended the original model of Schoups et al. (2005) to include the Corcoran clay and the confined aquifer beneath it, from which most groundwater is extracted. Following Belitz and Phillips (1995), no flow is assumed to occur between the confined aquifer and geological layers below it, at a depth of around 500 m. The extended model was partially recalibrated by adjusting hydraulic conductivities to match historically observed groundwater levels and soil salinity over the period 1941-1997.

3. Results

Table 1 gives an overview of the climate scenarios and projected atmospheric conditions for the period 2080-2099. For comparison, we have included historical climate data (denoted "H" in Table 1), and a scenario that assumes no climate change ("N"). The latter was obtained using statistical resampling of historical values, and resulting climate conditions differ slightly from historical conditions due to natural climate variability. The seven remaining scenarios represent different combinations of GHG emission scenarios, GCMs, and adaptation, with increased projected temperatures by the end of the 21st century. Climate change projections were differentiated between wet (W1 and W2) and dry (D1 through D4) scenarios We note that level of dryness correlates well with magnitude of projected warming (Figure 3a), though other studies with different GCM selections have not consistently showed this correlation (Cayan et al., 2008). The last scenario in Table 1 ("D4-IE") was included to assess consequences by increasing irrigation efficiency.

In the following, we discuss results for computed changes in irrigation water demand, irrigation water supply, and hydrologic response (Table 2, Figures 3 to 6). All scenarios account for retired land, i.e. land permanently taken out of production, as shown in Figure 1.

3.1. Irrigation water demand

Results in Table 2 (row 5) and Figure 3d indicate that total irrigation water demand is projected to decrease for the dry scenarios (D1 to D4) and increase for wet scenarios (W1 and W2), relative to the scenario without climate change (N). These results are counter-intuitive in that one would expect a greater need for irrigation water when rainfall is less, and vice versa. However, one must realize that all rainfall occurs in the off-season and annual irrigation water supply is inversely proportional to rainfall, thereby dictating cropped acreage and crop water requirements. Specifically, for the dry scenarios the reduced surface water supplies favor increased acreage of land fallowing, thereby reducing irrigation water demand (Table 2, Figure 3b), and a decreases in ET_c, despite a consistent increases in reference ET (Table 2, Figure 3c). Hence, the relationship between precipitation, surface water supply, and land fallowing drives irrigation water demand. This relationship is intuitive and is based on inverse correlations between precipitation and surface water supply projections of Vicuna et al. (2007), and between historical land fallowing and water supply for the water districts in the study area.

The projected decrease in ET_c (Figure 3c) contradicts the general belief that global warming will lead to an increase in crop transpiration in California (e.g., CA-DWR, 2006). The annual decrease in ET_c is a result of the accelerated crop development by the projected increased air temperatures (section 2.1). Since historical average daily temperatures were below the optimal range of 30-35°C, most crops will benefit from a modest temperature increases (2-5°C), resulting in faster crop development, thereby shortening the growing seasons and reducing annual crop water requirements. We note that we ignored the possibility of multiple cropping. As projected temperatures continue to rise, crop ET will increase due to an increase in ET_{ref}, as evidenced by the results for the warmest scenario D4 (Table 2, Figure 3c).

In addition to the projected climate change impacts, we note that irrigation water demands are already reduced by ongoing land retirement (Figure 3b), removing the most salt-affected areas from cultivation. Specifically, recent land retirement in our study area of about 60,000 acres caused a 16% decrease in irrigation water demand for our study area, irrespective of climate change (compare water demand entries for N with H scenarios in Table 2). The water supplies from these areas were transferred to the remaining agricultural lands in the district, outside our study area.

3.2. Irrigation water supply

Projections of surface water and groundwater supply also differentiate between wet and dry scenarios, and are largely determined by the inverse correlation between annual precipitation and surface water supplies (Vicuna et al. , 2007). Projected surface water supplies range from an increase of 14% for the wettest scenario (W2), to a decrease of -26% for the driest scenario (D4), relative to a no-climate-change scenario (Table 2; Figure 3d). Because of recent land retirements, surface water supplies are significantly reduced for all scenarios, including the no-climate-change scenario (Figure 3d).

Groundwater use for irrigation follows the opposite trend of surface water supplies (Figure 3d), as most pumping will occur in the driest scenarios (D4), to compensate for reduced surface water supplies. The model assumes that farmers will avoid water stress of all cropped lands, thereby supplementing available surface water supplies with groundwater pumping to satisfy all water demands. As one would expect, improvements in irrigation efficiency reduced the need for groundwater pumping (D4-IE scenario, Table 2 and Figure 3d). The reduced groundwater pumping (Table 2) for the wet scenarios is caused by the higher predicted rainfall amounts for those scenarios as compared to the no-climate change benchmark.

3.3. Hydrologic response

We evaluate climate change impacts of water and land use changes on the hydrologic system by simulating shallow water table extent (section 3.3.1), soil salinity (section 3.3.2), salt-affected crop yields (section 3.3.3), groundwater salinity (section 3.3.4), and land subsidence (section 3.3.5). Using the modified hydro-salinity model of

Schoups et al. (2005), we first reconstructed historical changes starting in 1940, and extended simulations through the 21st century for each climate change scenario. Whereas aggregate study area results are summarized in Table 2, time-series and spatial maps are presented in Figs. 4-6.

3.3.1. Shallow water tables

Figure 4 shows historical and projected changes in the area affected by shallow water tables, less than 2 m below land surface. As irrigated area increased during mid-century and imported surface water replaced locally-pumped groundwater as the main irrigation water source, groundwater levels rose throughout the 20th century (Figure 4, and Schoups et al., 2005). Shallow water tables mainly developed in downslope, low-lying areas (see Figure 1). Results in Table 2 and Figure 4 show significant variations between scenarios. Wet scenario (W1, W2) projections show an increase in shallow water table extent by 2100, whereas dry scenario simulations (D1 to D4) predict a decrease in shallow water table extent. The dry scenario results are caused by the decrease in surface water supplies, thereby causing increased groundwater pumping and lower groundwater levels by induced downward hydraulic gradients. The shallow groundwater level extent for the D4-IE scenario (fractional area of 0.16 in Figure 4) was much smaller than any of the others because of the assumed high irrigation efficiency of 90% and the relatively high pumping rate (Table 2). Shallow groundwater table is one of the most important hydrologic variables, as it enhances the contribution of capillary rise to soil evaporation, leading to soil and groundwater salinization in downslope areas.

3.3.2. Soil salinity

Historical and projected changes in the area of salt-affected soils, as defined by electrical conductivity (EC) values greater than 4 dS/m. Historical simulations by Schoups et al. (2005) showed the large decrease in soil salinity in the San Joaquin Valley, with saline soils decreasing from a fractional area of about 0.5 to about 0.3 (Figure 5), as the alluvial soils contained high salt content originally and were reclaimed by irrigation. Soil salinization increased in the late 1990's because of excess application of surface water, leading to rising water tables and drainage problems.

When comparing soil salinity with shallow groundwater level extent, salinity projections are much less variable between climate scenarios. There appears to be an upper limit of the areal extent of salt-affected soils, geographically constrained to the low-lying areas with clayey deposits in the north-eastern part of the study area (Figure 5), leading to poorly drained conditions. Additional areas of shallow water table extent (Figure 4) are not salinized, because of adequate drainage to deeper groundwater. Alternatively, part of the retired areas (Figure 1) remains salinized, as caused by regional shallow groundwater flow from upslope areas towards the retired agricultural lands. The largest decrease in salt-affected area was predicted for scenario D4-IE, as it exhibits the least shallow groundwater extent. Hence, source control through improvements in irrigation efficiency can be an effective management approach to reduce groundwater levels and soil salinity.

3.3.3. Crop yields

Apart from changes in salt-affected areas, we also considered the impact of soil salinity on crop production, as crop salt tolerance varies among crops and is not limited to

4 dS/m. Here, we present simulated yields for cotton (salt tolerant) and tomato (salt-sensitive), as affected by soil salinity, using the Maas-Hoffman function that relates relative yield to average root zone salinity (Maas, 1990). Whereas cotton yields were historically not affected by soil salinity (Table 2, Figure 6a), projected results for all climate scenarios indicate that soil salinity levels in salt-affected areas are expected to increase, reducing yield to 50% or more for about 20% of the study area by 2100. As expected, the wet scenarios with limited groundwater pumping predict the widest extend of yield reduction, and the scenario with technological adaptation projects (D4-IE) is the least affected (see also Figure 5). Our simulation results confirm that soil salinization will continue unless higher irrigation water efficiency management practices are widely used. Figure 6 also shows that the yield-reducing areas are mainly concentrated in the southern part of the study area, coinciding with the northern portion of Westlands Water District with shallow water tables and poor drainage. Though this area has already partly been retired from agricultural production (Figure 1), our results suggest that future land retirement may be necessary for areas further upslope as well.

Because of the increasing sensitivity to salinity stress, the area affected by tomato yield reduction is much larger (up to 30%), and is almost twice as big (Table 2 and Figure 6b) as for cotton. Results suggest that in some high saline areas, initial reclamation of soils by irrigation was likely necessary to allow tomato production. Furthermore, renewed soil salinization after the availability of surface water supply in the mid 20th century has affected tomato yields from the 1970's-1980's onwards, confirming anecdotal evidence by local farmers who indicated that tomato production has shifted upslope (towards the west). As many high-valued crops such as vegetables and fruit (melons, in particular) are also salt sensitive, the anticipated increase in future demand for such crops may require improved water and salt management practices in the study area.

3.3.4. Groundwater salinity

As determined by Schoups et al. (2005), the degradation of groundwater quality in the long-term may eventually jeopardize groundwater-based irrigated agriculture. Therefore, in addition to considering soil salinity, we also quantified salt loadings below the root-zone (Table 2). Differences in salt loading to groundwater between climate scenarios are related to groundwater pumping, with the highest salt loadings projected for the driest climate change scenario, D4. This is caused by (i) higher salinity of pumped groundwater compared to imported high quality surface water, and (ii) lower water tables induced by downward hydraulic gradients by groundwater pumping. Most of the salt leaching will occur for the well-drained soils in the western half of the study area (upslope), where soils are well drained. In the long-term, this leaching process, combined with the continued dissolution and transport of soil gypsum, will continue to increase groundwater salinity of underlying aquifers (Schoups et al., 2005). Excessive soil salinization in downslope areas in the eastern part of the study area is caused by groundwater discharge by regional lateral flow, resulting in upward salt fluxes from deeper groundwater into the root-zone.

3.3.5. Land subsidence

We included an estimate of potential land subsidence as part of the climate change analysis, considering inelastic compaction of sediments. For each climate change scenario, the simulation model computed hydraulic head values in the confined aquifer, in response to projected changes in groundwater pumping. Future occurrence of inelastic land subsidence was recorded when simulated confined heads fell below previously simulated minimum levels. This definition of inelastic compaction is only approximate, as it ignores the presence of residual pore pressure (Larson et al., 2001; Alley et al., 2002), potentially underestimating total subsidence. We use an inelastic storage coefficient of 10% (Domenico and Schwartz, 1998), i.e. 1 m of subsidence for each 10 m drop in head, to estimate total land subsidence in each grid cell over the period 2010-2099. Results show that land subsidence is projected to be very limited, with no subsidence for the wet and no-climate-change scenarios (Table 2). The driest D4 scenario with the largest groundwater pumping value projects subsidence in less than 1% of the irrigated area, for a total simulated subsidence of less than 30 cm.

4. Concluding Remarks

The sensitivity results presented provide insights into impacts of climate change on irrigated agriculture. Our analysis does not only apply to California, but can be extended to other irrigated regions in the world, as many have similar constraints regarding water supply and land degradation. Our conclusions about potential impacts of climate change on irrigated agriculture can be summarized as follows:

- Water demand: Demand projections for the 1,400 km^2 study region in the western San Joaquin Valley range from a decrease of 13% to an increase of 3% by the end of the 21st century. Reductions are largest in dry and warm scenarios, for which increased fallowing and decreased crop transpiration was projected, both leading to reductions in irrigation water demand. Our simulations showed that an increase in ET_{ref} for a warming climate is offset by a decrease in seasonal crop ET due to faster crop development. Though climate warming unexpectedly projected reduced seasonal crop water requirements, the resulting shorter growing seasons could make multiple cropping possible, thereby increasing annual irrigation water demand, perhaps beyond what can be supplied.

- Water supply: The impact of climate change on water supply ranges from a decrease of 26% to an increase of 14% towards the end of the 21st century. We assumed that groundwater pumping supplemented surface water supplies to meet total water demand, thereby resulting in a large range (factor of 5) in projected groundwater use values, among scenarios. It is important to realize that the uncertainty in surface water supply projections is very high, due to large variations in projected precipitation among climate scenarios.
- Shallow water tables and soil salinity: Despite the large variation in the spatial extent of projected shallow water tables, the total salt-affected area is predicted to remain fairly constant in the 21st century, irrespective of climate scenario. High soil salinity is limited to the eastern half of the study area that is flat and poorly drained. The western half of the study area contains topographic gradients and coarse alluvial soil deposits, which is why salinization due to rising water tables is unlikely to occur in those areas, irrespective of climate scenario.
- Crop productivity: All scenarios project an increase in soil salinity in downslope areas (eastern portion of the study area), resulting in reduction of both tomato and cotton yields. Although already a significant fraction of the low-lying areas has been retired from agricultural production, model simulations indicated that additional upslope areas could be affected. Therefore, if these additional lands

will not be drained in the future, additional land retirement may be required. Model results show that salinization will continue to occur, regardless of climate change. This is especially significant, realizing that economic analysis has shown that farmers will likely switch from salt tolerant crops (such as cotton) to high-value, salt-sensitive crops (such as tomato and melons), in the future.

- Groundwater salinity: Salt leaching to deeper groundwater is most significant for the dry climate change scenarios, for which groundwater use is greatest. Groundwater irrigation generates the highest groundwater salinity, as salinity increases by recycling of already salinized groundwater, combined with gypsum dissolution. Hence, although groundwater pumping may reduce shallow groundwater extent, thereby preventing excessive soil salinization, irrigation with saline groundwater accelerates groundwater salinization. We realize that the time scales of these two processes are different, with soil salinization being controlled and managed over time scales of years and decades, whereas deep groundwater salinization occurs over time scales of decades to hundreds of years.
- Land subsidence: Land subsidence is projected to be very limited, even for the driest climate scenario, using historical subsidence and groundwater pumping simulations. However, we realize that direct modeling of pore pressures and subsidence calculations are needed to more accurately assess the future occurrence of land subsidence if groundwater pumping is increased.
- Technological adaptation: Among the simulated scenarios, we considered a technological adaptation by improving irrigation efficiency to 90%. Such an adaptation could effectively mitigate many projected adverse effects. Increasing irrigation efficiency would reduce groundwater pumping, irrigation water

demand, groundwater recharge, and soil salinity (both extent and level of salinity), thereby decreasing the need for land retirement.

In conclusion, the greatest threat to agricultural sustainability in the study area appears to be the continued salinization of downslope areas, jeopardizing crop production and requiring future land retirement. Technological adaptations, such as increasing irrigation efficiency, may mitigate these effects. Future work should consider additional scenarios, and evaluate the vulnerability of the system to increased groundwater pumping. This would require addressing economic profitability of irrigated agriculture, for example, to include pumping costs and crop yield reduction by salinity. Also, more work is needed on quantifying the uncertainties of the projected impacts, including climate projections and the hydro-salinity model. We also conclude that many of the simulated adverse effects, such as soil salinization, are caused by regional groundwater dynamics of the hydrologic system in the study area, irrespective of climate change. It is therefore important to include such hydrologic dynamics in any impact assessment, as they may be as important as potential climate impacts.

5. Acknowledgments

The research was made possible through funding by the UC Water Resources Center Project SD011. We also thank Dr. Rick Snyder of the Department of Land, Air and Water Resources of UC Davis for his contributions on estimating evapotranspiration.

6. References

Ainsworth, E.A., and A. Rogers (2007), The response of photosynthesis and stomatal conductance to rising CO_2: mechanisms and environmental interactions, Plant, Cell and Environment, 30:258–27.

Alley, W.A., R.W. Healy, J.W. LaBaugh, and T.E. Reilly (2002), Flow and storage in groundwater systems, Science, 296, 1985-1990.

ASCE-EWRI (2004), The ASCE standardized reference evapotranspiration equation, Technical Committee report to the Environmental and Water Resources Institute of the American Society of Civil Engineers from the Task Committee on Standardization of Reference Evapotranspiration, Reston ,VA, USA. 173 pp.

Barnett, T.P., J.C. Adam, and D.P. Lettenmaier, 2005, Potential impacts of a warming climate on water availability in snow-dominated regions, Nature, 438, 303-309.

Barnett, T.P., et al. (2008), Human-induced changes in the hydrology of the western United States, Science, 319, 1080-1083.

Belitz, K., and S.P. Phillips (1995), Alternative to agricultural drains in California's San Joaquin Valley: results of a regional-scale hydrogeologic approach. Water Resour. Res. 31 (8), 1845–1862.

Boote, K.J., J.W. Jones, and G. Hoogenboom (1998), Simulation of crop growth: CROPGRO model, p.651–692. In: R. M. Peart and R. B. Curry (eds.), Agricultural systems modeling and simulation. Marcel Dekker, NewYork.

CA-DWR (2006), Progress on incorporating climate change into planning and management of California's water resources, Technical Memorandum Report, California Department of Water Resources, Sacramento, CA, July 2006, 339 pp.

CA-EPA (2006), Climate action team report to Governor Schwarzenegger and the Legislature, California Environmental Protection Agency, Sacramento, CA, March 2006, 110 pp.

Cayan, D.R., E.P. Maurer, M.D. Dettinger, M. Tyree and K. Hayhoe, 2008, Climate change scenarios for the California region, *Climatic Change*, Vol. 87, Suppl. 1, 21-42 doi: 10.1007/s10584-007-9377-6.

Cline, W.R. (2007), Global warming and agriculture: impact estimates by country, Peterson Institute for International Economics, July 2007, 250 pp.

Crafts-Brandner, S.J., and M.E. Salvucci (2000), Rubisco activase constrains the photosynthetic potential of leaves at high temperature and CO_2, PNAS, 97(24), 13430-13435.

Döll, P. (2002), Impact of climate change and variability on irrigation requirements: a global perspective, Climatic Change, 54, 269-293.

Döll and Siebert, 2002., Global modeling of irrigation water requirements, Water Resour Res. 38:8, DOI 10.1029/2001WR000355

Domenico, P.A., and W. Schwartz (1998), Physical and chemical hydrogeology, second edition, Wiley.

Galloway, D., D.R. Jones, and S.E. Ingebritsen (1999), Land Subsidence in the United States, United States Geological Survey, Circular 1182, 177 pp.

Ghassemi F., A.J. Jakeman, and H.A. Nix. 1995. Salinization of Land and Water Resources: Human Causes, Extent, Management & Case Studies. Univ. of New South Wales Press Ltd. Sydney, Australia.

Gordon, C., C. Cooper, C.A. Senior, H.T. Banks, J.M. Gregory, T.C. Johns, J.F.B. Mitchell, and R.A. Wood (2002), The simulation of SST, sea ice extents and ocean heat transports in a version of the Hadley Centre coupled model without flux adjustments, Climate Dynamics, 16, 147-168.

Hayhoe, K., D.R. Cayan, C.B. Field, P.C. Frumhoff, E.M. Maurer, N. Miller, S. Moser, S. Schneider, K. Cahill, E. Cleland, L. Dale, R. Drapek, R.M. Hanemann, L. Kalkstein, J. Lenihan, C. Lunch, R. Neilson, S. Sheridan, and J. Verville (2004), Emissions pathways, climate change, and impacts on California, Proceedings of the National Academy of Sciences, 101(34), 12422–12427.

IPCC (2007), Climate Change 2007: Synthesis Report, Contribution of Working Groups I, II and III to the Fourth Assessment Report of the Intergovernmental Panel on Climate Change [Core Writing Team, Pachauri, R.K and Reisinger, A. (eds.)], *IPCC*, Geneva, Switzerland, 104 pp.

Kalnay, E., et al. (1996), The NCEP/NCAR 40-year reanalysis project, Bull. Amer. Meteor. Soc., 77, 437-471.

Kimball, B.A., K. Kobayashi, and M. Bindi (2002), Responses of agricultural crops to free-air CO_2 enrichment, Advances in Agronomy, 77, 293-368.

Kundzewicz, Z.W., L.J. Mata, N.W. Arnell, P. Döll, P. Kabat, B. Jiménez, K.A. Miller, T. Oki, Z. Sen and I.A. Shiklomanov, 2007, Freshwater resources and their management. Climate Change 2007: Impacts, Adaptation and Vulnerability. Contribution of Working Group II to the Fourth Assessment Report of the Intergovernmental Panel on Climate Change, M.L. Parry, O.F. Canziani, J.P. Palutikof, P.J. van der Linden and C.E. Hanson, Eds., Cambridge University Press, Cambridge, UK, 173-210.

Larson, K.J., H. Basagaoglu, and M.A. Marino (2001), Prediction of optimal safe groundwater yield and land subsidence in the Los Banos-Kettleman City area, California, using a calibrated numerical simulation model, Journal of Hydrology, 242(1-2), 79–102.

Lobell, D.B., C.B. Field, K.N. Cahill, and C. Bonfils (2006), Impacts of future climate change on California perennial crop yields: Model projections with climate and crop uncertainties, Agricultural and Forest Meteorology, 141, 208–218.

Long, S.P., E.A. Ainsworth, A.D.B. Leakey, J. Nösberger, and D.R. Ort. 2006. Food for Thought: Lower-than-expected crop yield stimulation with rising CO2 concentrations. Science 312:1918-1921.

Maas, E.V. (1990), Crop salt tolerance, In: K.K. Tanji (ed.), Agricultural salinity assessment and management, ASCE Manuals and Reports on Engineering Practice no. 71, Am. Soc. Civil Eng., New York.

Maurer, E.P., A.W. Wood, J.C. Adam, D.P. Lettenmaier, and B. Nijssen (2002), A long-term hydrologically-based dataset of land surface fluxes and states for the conterminous United States, J. Climate 15(22), 3237-3251.

Maurer, E.P., 2007, Uncertainty in hydrologic impacts of climate change in the Sierra Nevada, California under two emissions scenarios, Climatic Change, Vol. 82, No. 3-4, 309-325, doi: 10.1007/s10584-006-9180-9.

Milly, P.C.D., K.A. Dunne, and A.V. Vecchia, 2005, Global pattern of trends in streamflow and water availability in a changing climate, Nature, 438, 347-350.

Moench, M. (2004), Groundwater: the challenge of monitoring and management, In: P. Gleick. (Ed.), The World's Water 2004-2005, The Biennial Report on Freshwater Resources, Island Press, Washington D.C., USA, pp. 79-100.

Panofsky, H. A. and G. W. Brier: Some Applications of Statistics to Meteorology. The Pennsylvania State University, 224 pp, 1968

Ritchie, J. T., and D. S. NeSmith (1991), Temperature and crop development, p.5–29. In: J. Hanks and J. T. Ritchie (eds.), Modeling plant and soil systems. Agron. Monogr. 31, ASA, CSSA, and SSSA. Madison, WI.

Rosegrant, M.W., and S.A. Cline (2003), Global food security: challenges and policies, Science, 302, 1917-1919.

Rozenzweig, C. and D. Hillel. 1998. Climate change and the global harvest – Potential impacts of the greenhouse effect on agriculture. Oxford University Press.

Schlenker, W., W. Hanemann, and A. Fisher (2007), Water availability, degree days, and the potential impact of climate change on irrigated agriculture in California. Climatic Change, 81(1):19-38.

Schoups, G., J.W. Hopmans, C.A. Young, J.A. Vrugt, W.W. Wallender, K.K. Tanji, and S. Panday (2005), Sustainability of irrigated agriculture in the San Joaquin Valley, California, PNAS, 102(43), 15352-15356.

Schoups, G., C.L. Addams, J.L. Minjares, and S.M. Gorelick (2006), Sustainable conjunctive water management in irrigated agriculture: Model formulation and application to the Yaqui Valley, Mexico, Water Resour. Res., 42, W10417, doi:10.1029/2006WR004922.

Schmidhuber, J., and F.N. Tubiello, 2007, Global food security under climate change, Proc. Nat. Ac. Sci., 104(50), 19703-19708.

Sherif, M., and V. Singh, 1999, Effect of climate change on sea water intrusion in coastal aquifers, Hydrol. Proc., 13, 1277-1287.

Snyder, R.L., B.J. Lanini, D.A. Shaw, and W.O. Pruitt (1989), Using reference evapotranspiration and crop coefficients to estimate crop evapotranspiration for agronomic crops, grasses, and vegetable crops. California Department of Water Resources, Leaflet 21427, Sacramento, CA, pp. 1-12.

Thornton, P.E., H. Hasenauer, and M.A. White (2000), Simultaneous estimation of daily solar radiation and humidity from observed temperature and precipitation: an application over complex terrain in Austria, Agric. For. Meteor., 104, 255-271.

Van Rheenen, N.T., Wood, A.W., Palmer, R.N., and Lettenmaier, D.P.: 2004, Potential implications of PCM climate change scenarios for California hydrology and water resources, *Climatic Change* 62, 257-281.

Vicuna, S., E.P. Maurer, B. Joyce, J.A. Dracup, and D. Purkey (2007), The sensitivity of California water resources to climate change scenarios, Journal of the American Water Resources Association, 43(2): 482-498.

Vlek, P.L.G., D. Hillel, and A.K. Braimoh (2008), Soil degradation under irrigation, In: A.K. Braimoh and P.L.G. Vlek (eds.), Land use and soil resources, Springer, p. 101-119.

Washington, W.M., J.W. Weatherly, G.A. Meehl, A.J. Semtner, T.W. Bettge, A.P. Craig, W.G. Strand, J. Arblaster, V.B. Wayland, R. James, and Y. Zhang (2000), Parallel climate model (PCM) control and transient simulations, Climate Dynamics, 16(10/11), 755-774.

Wood, A.W., E.P. Maurer, A. Kumar, and D.P. Lettenmaier (2002), Long range experimental hydrologic forecasting for the eastern U.S., J. Geophys. Res. 107 (D20): 4429.

Wood, A.W., Leung, L.R., Sridhar, V., and Lettenmaier, D.P.: 2004, 'Hydrologic implications of dynamical and statistical approaches to downscaling climate model outputs', *Climatic Change* 62, 189-216.

Table 1. Overview of climate change scenarios. Projected temperature and precipitation are average values for the end of the 21st century (2080-2099), based on bias-corrected and spatially downscaled GCM output. Historical data are for the period 1976-1995.

Scenario label	**GCM**	**SRES emission scenario**	**Technological adaptation**	**Atmospheric CO_2 (ppm)**	**Air temperature (°C)**	**Precipitation (m)**
H	Historical		-	347	17.1	0.21
N	No climate change		-	347	17.6	0.20
W1	PCM	B1	-	544	19.2	0.24
W2	PCM	A2	-	775	20.2	0.24
D1	PCM	A1fi	-	885	20.8	0.18
D2	HadCM3	B1	-	544	20.9	0.18
D3	HadCM3	A2	-	775	22.2	0.17
D4	HadCM3	A1fi	-	885	23.5	0.13
D4-IE	HadCM3	A1fi	IE*	885	23.5	0.13

* Uniform increase in irrigation efficiency to 90%, from current efficiencies ranging from 65 to 80%.

Table 2. Climate change impacts on water supply, water demand, and hydrology. Values represent averages or totals over the entire study area and over a 20-year period. Refer to Table 1 for scenario labels and climate characteristics. Minimum and maximum values for each variable are underlined.

Scenario	**H**	**N**	**W1**	**W2**	**D1**	**D2**	**D3**	**D4**	**D4-IE**
Time period	**1976-1995**	**2080-2099**	**2080-2099**	**2080-2099**	**2080-2099**	**2080-2099**	**2080-2099**	**2080-2099**	**2080-2099**
Water demand									
Reference ET (m)	1.49	1.53	1.52	1.57	1.60	1.62	1.65	1.73	1.73
Crop ET (m) [(a)], scenario 1	0.58	0.58	0.54	0.54	0.53	0.55	0.55	0.60	0.60
Crop ET (m) [(a)], scenario 2	0.58	0.60	0.56	0.55	0.54	0.57	0.56	0.60	0.60
Non-cultivated land [(c, d)]	0.15	0.31	0.30	0.31	0.33	0.34	0.34	0.34	0.34
Water demand (MCM) [(b)]	831	694	702	717	617	620	634	664	601
Water supply									
Surface water use (MCM) [(b)]	744	588	652	673	498	462	469	433	433
Groundwater use (MCM) [(b)]	87	105	50	44	119	158	165	232	168
Hydrologic response									
Shallow water tables [(c)]	0.40	0.39	0.53	0.55	0.29	0.24	0.25	0.23	0.11
Salt-affected soils [(c)]	0.32	0.47	0.47	0.49	0.46	0.46	0.46	0.47	0.37
Cotton yield < 50% [(c)]	0.00	0.18	0.19	0.22	0.17	0.16	0.15	0.15	0.10
Tomato yield < 50% [(c)]	0.08	0.31	0.32	0.34	0.29	0.29	0.27	0.27	0.18
Salt loading to groundwater (million tons)	5.47	2.37	2.37	1.12	2.77	3.39	3.55	4.74	4.67
Renewed land subsidence [(c)]	N/A	0.01	0.00	0.00	0.00	0.00	0.00	0.00	0.00

[a] This is a weighted average over all crops, with weights proportional to crop acreages. Results are shown for two scenarios. Scenario 1 corresponds to an assumption of no change in cropping patterns. Scenario 2 assumes a demand-driven shift to high-value crops, such as vegetables and fruits (Howitt et al., 2003). Results for water demand, supply and hydrologic responses are for scenario 1.

[b] Total water volume in Million Cubic Meter (MCM).

[c] Fraction of total land area. Shallow water table are less than 2 m below land surface. Salt-affected soils have an EC_e greater than 4 dS/m.

[d] Includes non-agricultural areas (4% of total land area) and, for future years, retired agricultural land (18% of total land area).

Figure Captions

Figure 1 (a) Location of study area and model domain in the western San Joaquin Valley, California; (b) Detailed view of model domain, showing irrigation districts (as jagged lines) and two dark areas where land is retired from agricultural production as of 2006. Grey shades indicate land elevation, with lighter shades having higher elevation. Regional groundwater flow follows topographic gradients, i.e. south-west to north-east.

Figure 2 Validation results for reference ET estimation. "Diamonds" are data for temperature, precipitation, and reference ET measured at a local CIMIS weather station in the study area. "Squares" are (i) gridded data of precipitation and temperature from Maurer et al. (2002) for the grid point at the center of the study area, and (ii) calculated values of reference ET based on these temperature and precipitation data, using the method of Thornton et al. (2000).

Figure 3 (a) Precipitation and temperature for various climate scenarios listed in Table 1, and resulting projections in land use (b), reference ET and crop ET (c), and irrigation water demand and supply (d). Reported values are totals for the entire study area and averaged in time for the period 2080-2099 (except for historical conditions denoted by "H", which represents the period 1976-1995). BCM = Billion Cubic Meter.

Figure 4 Historical and projected extent of shallow groundwater areas: time-series and spatial maps for three scenarios, i.e. N (no climate change), W2 (wettest scenario), and D4-IE (driest scenario). Shallow water tables are less than 2 m below land surface. Solid lines are simulations, and open symbols are observations in May (squares), July (diamonds), or October (triangles).

Figure 5 Historical and projected extent of salt-affected areas: time-series and spatial maps for three scenarios, i.e. N (no climate change), W2 (wettest scenario), and D4-IE (driest scenario). Salt-affected soils have an EC_e greater than 4 dS/m. Solid lines are simulations, and open symbols (triangles) are observations.

Figure 6 Historical and projected extent of areas where (a) cotton and (b) tomato yield is reduced by 50% or more due to salt accumulation: time-series and spatial maps for three scenarios, i.e. N (no climate change), W2 (wettest scenario), and D4-IE (driest scenario). Yield reductions are more severe for darker shades.

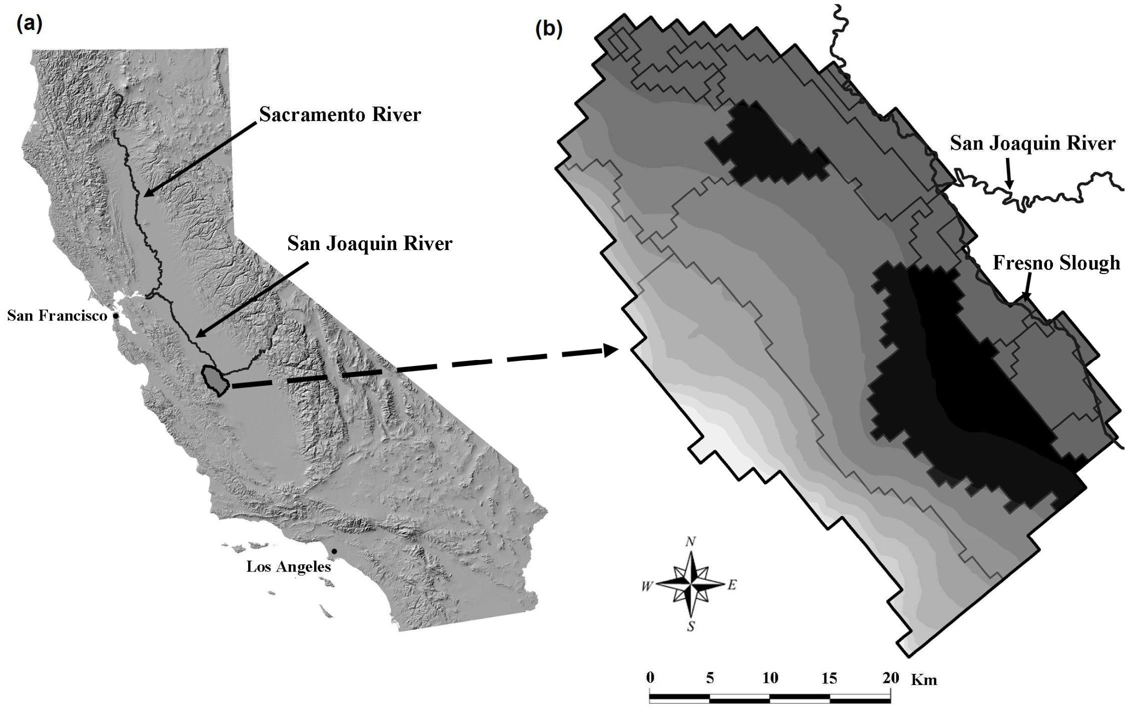

Figure 1 (a) Location of study area and model domain in the western San Joaquin Valley, California; (b) Detailed view of model domain, showing irrigation districts (as jagged lines) and two dark areas where land is retired from agricultural production as of 2006. Grey shades indicate land elevation, with lighter shades having higher elevation. Regional groundwater flow follows topographic gradients, i.e. south-west to north-east.

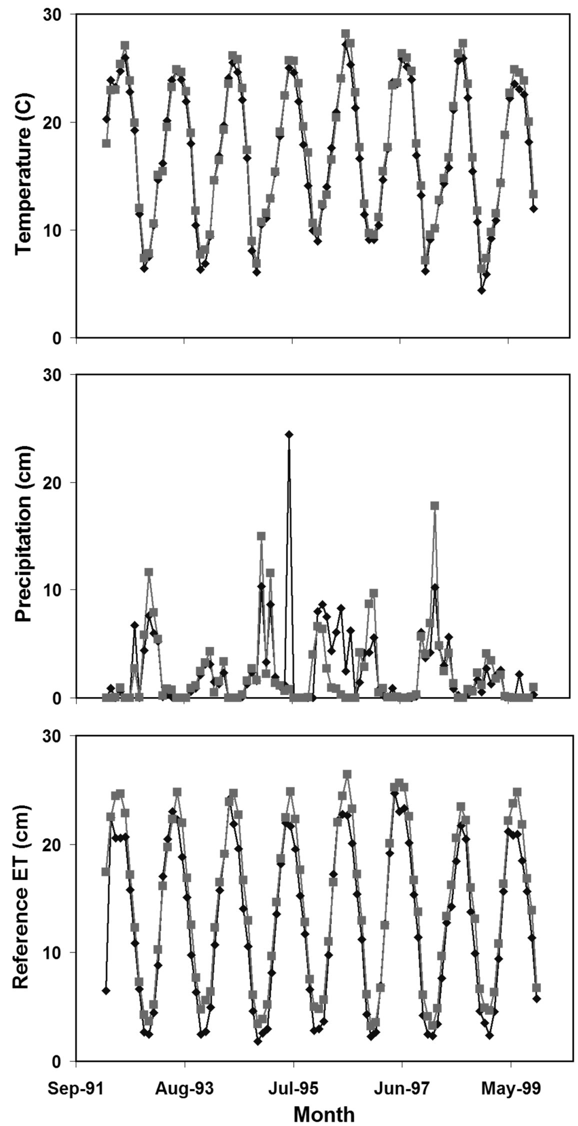

Figure 2 Validation results for reference ET estimation. "Diamonds" are data for temperature, precipitation, and reference ET measured at a local CIMIS weather station in the study area. "Squares" are (i) gridded data of precipitation and temperature from Maurer et al. (2002) for the grid point at the center of the study area, and (ii) calculated values of reference ET based on these temperature and precipitation data, using the method of Thornton et al. (2000).

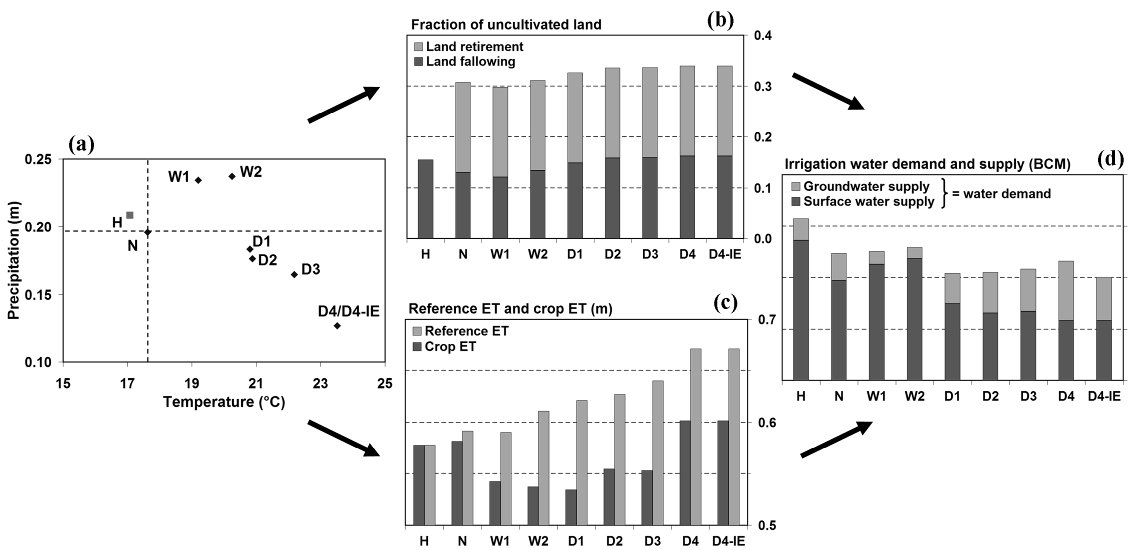

Figure 3 (a) Precipitation and temperature for various climate scenarios listed in Table 1, and resulting projections in land use (b), reference ET and crop ET (c), and irrigation water demand and supply (d). Reported values are totals for the entire study area and averaged in time for the period 2080-2099 (except for historical conditions denoted by "H", which represents the period 1976-1995). BCM = Billion Cubic Meter.

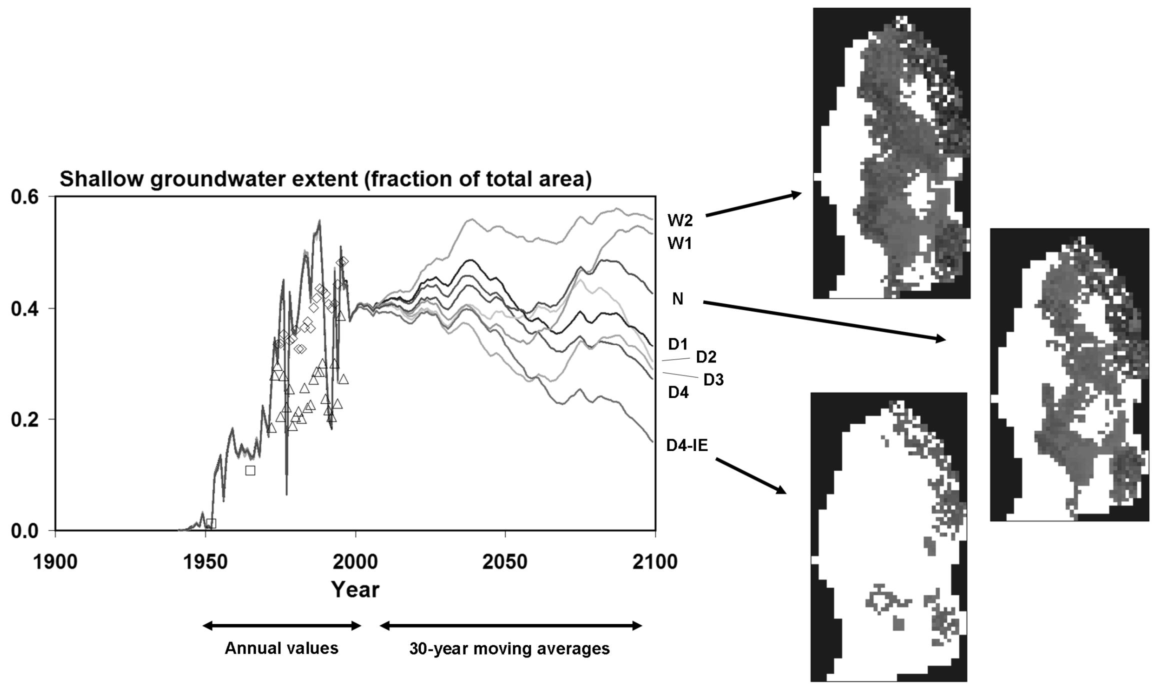

Figure 4 Historical and projected extent of shallow groundwater areas: time-series and spatial maps for three scenarios, i.e. N (no climate change), W2 (wettest scenario), and D4-IE (driest scenario). Shallow water tables are less than 2 m below land surface. Solid lines are simulations, and open symbols are observations in May (squares), July (diamonds), or October (triangles).

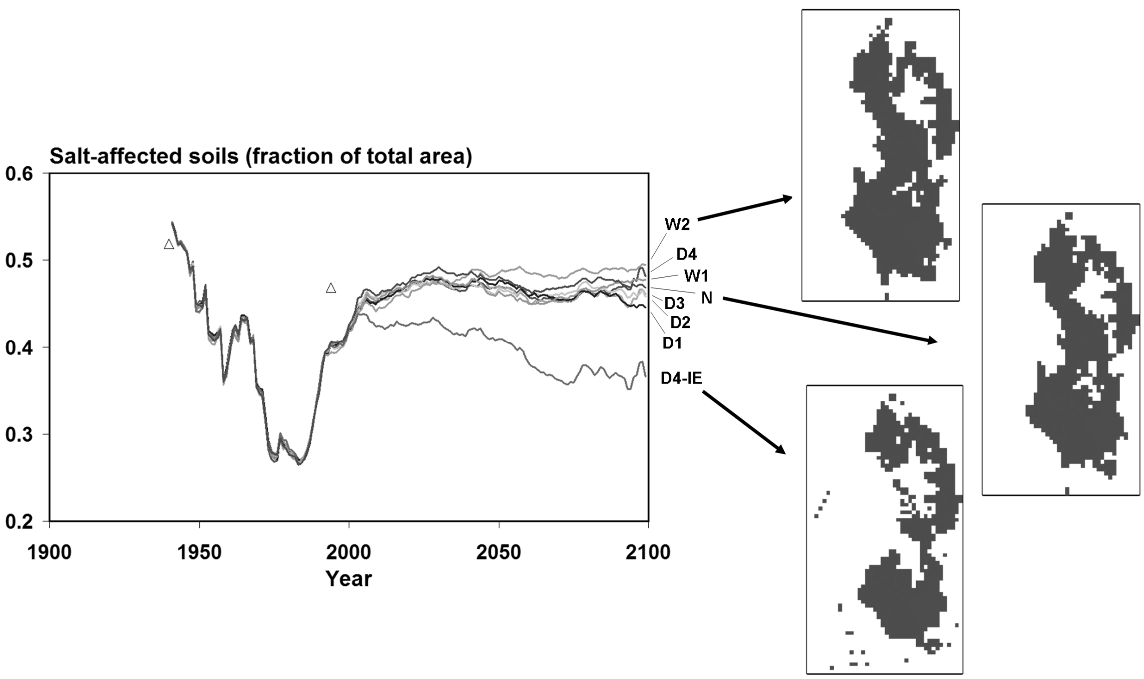

Figure 5 Historical and projected extent of salt-affected areas: time-series and spatial maps for three scenarios, i.e. N (no climate change), W2 (wettest scenario), and D4-IE (driest scenario). Salt-affected soils have an EC_e greater than 4 dS/m. Solid lines are simulations, and open symbols (triangles) are observations.

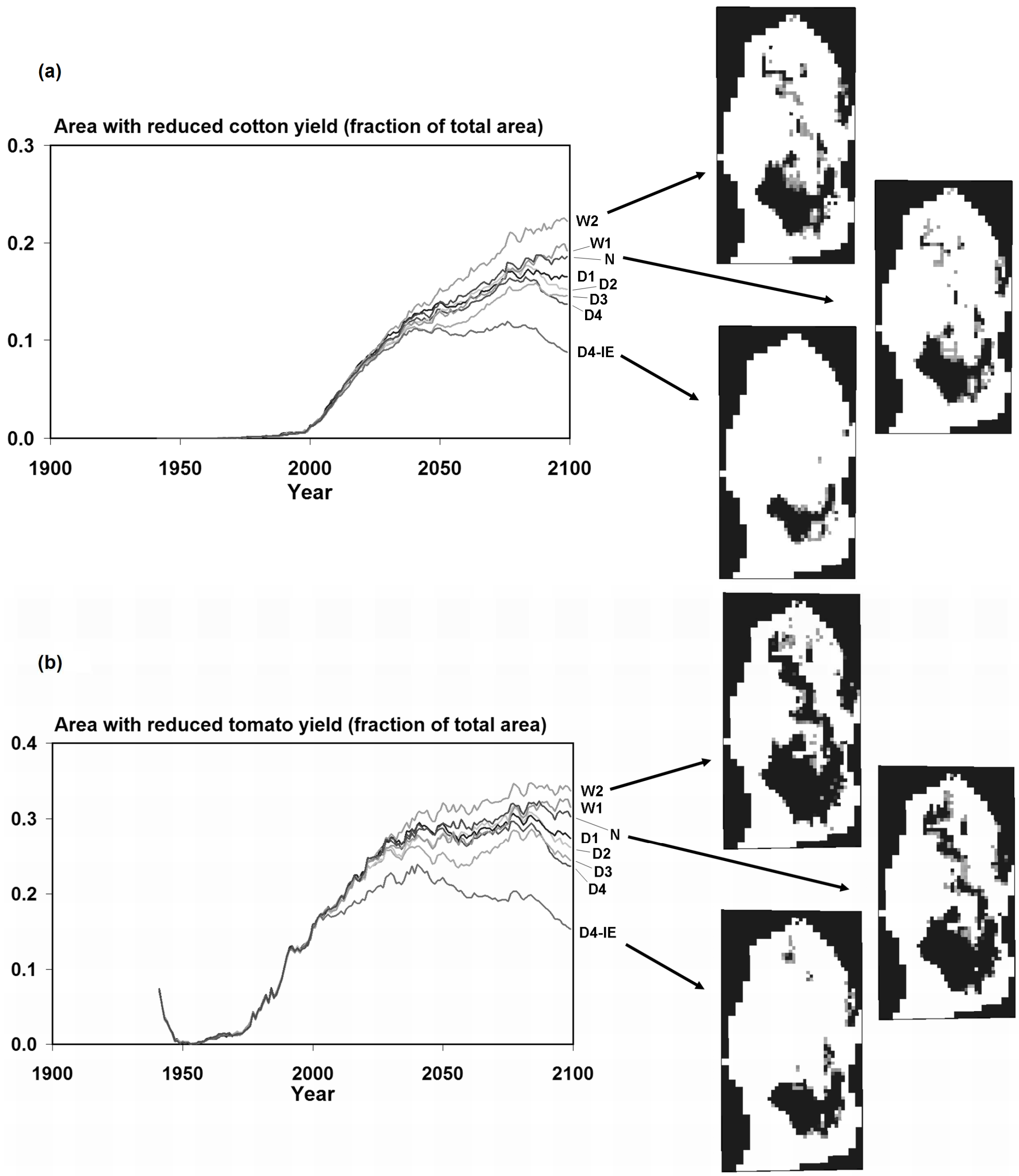

Figure 6 Historical and projected extent of areas where (a) cotton and (b) tomato yield is reduced by 50% or more due to salt accumulation: time-series and spatial maps for three scenarios, i.e. N (no climate change), W2 (wettest scenario), and D4-IE (driest scenario). Yield reductions are more severe for darker shades.